JOURNAL OF APPLIED ELECTROCHEMISTRY 20 (1990) 625–629

The addition of aluminium oxide to the nickel anodes of a molten carbonate fuel cell

L. SUSKI, J. WYRWA

Institute of Physical Chemistry of the Polish Academy of Sciences, Molten Salts Laboratory, 30-059 Krakow, al. Mickiewicza 30, Poland

Received 22 December 1987; revised 14 October 1989

Al_2O_3 was added to porous Ni + Ag and Ni electrodes which were subsequently tested as anodes in a molten carbonate fuel cell. It has been shown that this component increases the specific inner surface of the anodes and improves their polarization characteristics. The correlation between these parameters has been discussed in terms of a model proposed previously [8, 9]. The good performance of the cells with electrolytes manufactured using Al_2O_3-derived material as a matrix may be correlated with the influence of this compound on the inner surface area of the nickel porous electrode.

Nomenclature

A, B	linear relationship parameters
d	density of electrode material
I	current density
L	electrode thickness
S	internal surface of electrode per unit volume
S_w	internal surface of electrode per unit weight
Z	total electrode impedance per unit area of electrode
Z_F	$\eta(I)$ function slope at zero current
η	overpotential
κ_E^{eff}, κ_M^{eff}	effective specific electrolyte and electrode conductivities, respectively

1. Introduction

In an electrochemical power generator operating on the principle of the molten carbonate fuel cell (MCFC) so called 'matrix' or 'paste' electrolytes are used in which some refractory oxides constitute the solid 'matrix' for the molten carbonate phase. In state-of the-art MCFC devices $LiAlO_2$ is applied for this purpose [1, 2]. This compound may be produced in the reaction of solid Al_2O_3 with liquid lithium carbonate. As early as 1969, in the fundamental research on the MCFC by Broers and Ballegoy [3] it was shown that $LiAlO_2$ as a solid component of the electrolyte tiles, provides much better cell performance than that obtained with MgO, which was used in the preliminary studies [4]. Cells with electrolytes prepared using aluminium oxide give higher and more stable power densities than those with MgO as the solid component of the electrolytic tiles [4].

The superiority of $LiAlO_2$-based 'matrix' or 'paste' electrolytes with respect to the MgO-based ones has been commonly recognised but, according to our knowledge, no precise explanation of this effect has been given. Some preliminary results reported by Broers and Ballegoy [3], who mentioned solubility of MgO in molten carbonates, do not elucidate all the aspects of this complex problem.

In order to investigate the influence of the Al_2O_3-derived compounds on the performance of MCFC electrodes, independently of the electrolyte used, we have tested small cells of this type using 'matrix' electrolytes with MgO as a solid component and porous anodes prepared on nickel and doped with controlled amounts of aluminium oxide. In this way the role of this component in the total electrocatalytic activity of the MCFC anodes has been studied.

2. Experimental details

2.1. *Description of the cell*

A schematic cross-section of the cell is presented in Fig. 1. The overpotential of the anode 1, was controlled with respect to the nickel foil reference electrode 2, inserted in the anodic compartment of the cell. The cell body 3, was made from a refractory chromium containing steel. It was insulated from the electrolytic tile 4, by a ring of mica 5. The porous silver cathode 6, was inserted on the lower side of the electrolytic tile. The latter consisted of a disc of MgO (50 mm in diameter and 4 mm thick) with 40% porosity, saturated with the $48\,Li_2CO_3 + 52\,Na_2CO_3$ eutectic mixture.

A gas mixture of the elementary composition C-11, H-72 and O-17 atom percent was supplied to the anodic compartment of the cell, whereas the cathodic gas composition was: air-71, CO_2-29 mole percent, The open circuit voltage (OCV) of this cell at the temperature of the experiments (850 K) was 1.040–1.050 V, in accordance with the EMF of the respective reversible cell [5].

0021-891X/90 $03.00 + .12

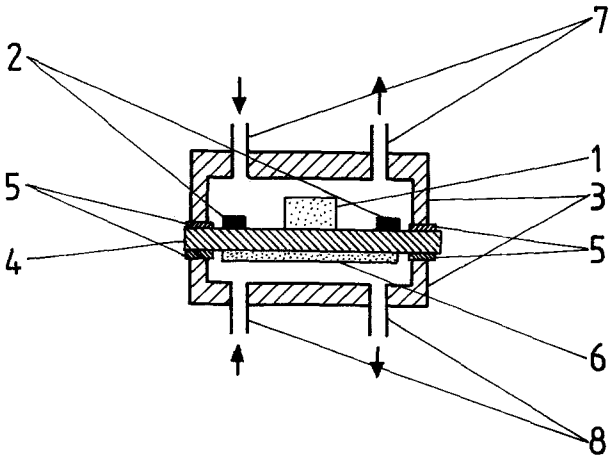

Fig. 1. Schematic cross-section of the cell. 1, Porous anode under investigation; 2, Ni-foil-reference electrode; 3, cell body; 4, electrolytic tile MgO_{solid} + (Li, $Na)_2CO_3$ eut.; 5, mica insulation; 6, porous Ag counter electrode; 7, CHO-fuel inlet/outlet; 8, air + CO_2-oxidant inlet/outlet.

2.2. *Preparation of the electrodes*

Both anodes and cathodes were prepared by pressing and sintering metallic powders or their mixtures, containing NH_4HCO_3 as the fluffing component. The cathodes were prepared from Ag powder of 3 μm medium particle size and were 30 mm in diameter and 0.5 mm thick. Two kinds of anodes were prepared: (1) from a 1 : 1 mole mixtures of Ni + Ag powders of 30–40 μm particle size: and (2) from the same fraction of the pure Ni powder.

The pressing parameters were: (1) 9.81×10^3 and (2) 12.75×10^3 N cm^{-2}, respectively. The sintering process was carried out in a pure hydrogen atmosphere. The anodes prepared in this way were 16 mm in diameter, to enable high current densities to be reached without excessive polarisation of the larger silver cathodes, and as much as 6 mm thick, so as to facilitate uniform doping with Al_2O_3.

The doping of these anodes with Al_2O_3 was carried out in two ways: (1) by saturation of the electrode with determined volumes of $Al(NO_3)_3$ solution of different concentrations, followed by a baking process; and (2) by an addition of a determined amount of Al_2O_3 to the Ni + Ag powder before the preparation of the electrode.

2.3. *Determination of the parameters of the anode porous structure*

The specific inner surface of the anodes, prepared according to the above procedures, was determined by the BET method using a Quantosorb device. The distributions of the sizes of the metallic particles containing elementary Ni, Ag and Al, in the anodes, before and after they had been used in the cells, were determined using a CAMECA MS 46 X-ray microanalyzer. The grain sizes were calculated from the distances among the reflected radiation peaks obtained in the X-ray scan over the studied surface area.

2.4 *The measurements of anode polarization*

The cells were assembled as shown in Fig. 1 and heated in an electric furnace to 850 K and the appropriate gas mixtures were supplied to both anodic and cathodic compartments with a flow rate of 50 dm^3 h^{-1}. When correct OCV values had been established and the electrical potential differences between the electrodes under study and the reference Ni electrodes did not exceed 5 mV, the polarization measurements were carried out by means of a stepwise 0.05 V increase and/or decrease of the anode overpotential within the limits 0 to + 0.2 V and recording the respective steady-state current values.

3. Results

In the preparation of the porous anodes and in the electrochemical experiments special attention was paid to the reproducibility of the results obtained. In order to satisfy this condition at least four electrodes of the same composition were prepared, two of which were used in two independent polarization experiments in the cell the other two being subject to two specific inner surface determinations and X-ray investigations. In some cases, however, 5 to 8 electrodes of the same composition were prepared and studied.

In all experiments a linear dependence of the current density on the anodic overpotential was found within the limits of 0.2 V with good approximation, in accordance with the respective polarization curves reported in the literature [6]. This fact enabled us to characterize the electrochemical properties of the given electrode by one parameter only: the total specific impedance which may be calculated from the relation

$$I(\eta) = \left(\frac{1}{Z}\right) \times \eta, \qquad (1)$$

as dependent on the given anodic overpotential. The overpotentials were not corrected for ohmic drop.

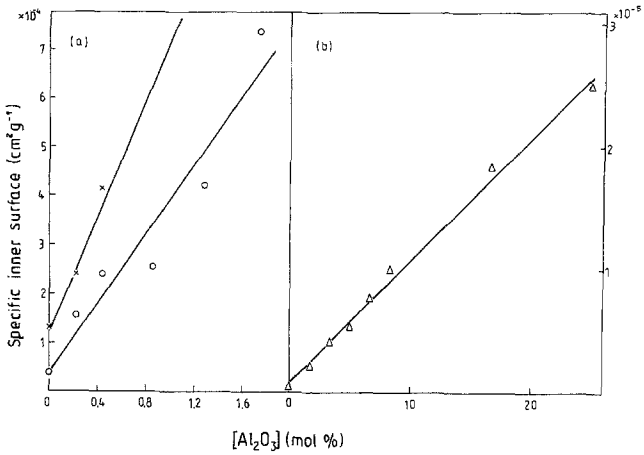

Fig. 2. BET specific inner surface areas of electrodes as dependent on Al_2O_3 concentrations. (a) electrodes doped by saturation with Al-ions solutions: x — Ni electrodes, o — Ni + Ag electrodes; (b) Ni + Ag electrodes doped by mixing metallic powders with solid Al_2O_3:—— least squares line.

Table 1. Compositions, specific inner surface areas and total impedances of the investigated electrodes: Electrodes 2, 3, 5 . . . 10-saturated with $Al(NO_3)_3$ solutions; electrodes 11 . . . 17-Al_2O_3 mixed to metal powder before sintering

Electrode		Specific inner surface area (S_u) ($cm^2\,g^{-1} \times 10^{-4}$)				Total impedance (Z) ($\Omega\,cm^2$)			
No.	Composition (mole percents)								
1	Ni	1.33	1.30	1.32	1.32	4.169	3.641	3.678	
2	Ni + 0.22% Al_2O_3	2.3	2.5			3.000	2.846		
3	Ni + 0.43% Al_2O_3	4.07	4.2			2.598	2.413		
4	Ni + Ag	0.40	0.39	0.38	0.39	2.708	2.858	2.777	2.788
5	Ni + Ag + 0.22% Al_2O_3	1.57	1.52			2.412	2.588	2.450	
6	Ni + Ag + 0.43% Al_2O_3	2.40	2.37			2.108	2.193		
7	Ni + Ag + 0.86% Al_2O_3	2.85	2.17	2.60		2.196	2.097	2.033	
8	Ni + Ag + 1.29% Al_2O_3	4.10	4.27			1.818	1.682		
9	Ni + Ag + 1.72% Al_2O_3	7.50	7.23	7.30		1.807	1.902	1.707	
10	Ni + Ag + 1.98% Al_2O_3	5.12	5.21			1.375	1.513	1.610	
11	Ni + Ag + 1.66% Al_2O_3	2.07	2.05			1.983	1.797		
12	Ni + Ag + 3.32% Al_2O_3	4.05				1.814	1.868		
13	Ni + Ag + 4.98% Al_2O_3	5.52				1.531	1.384		
14	Ni + Ag + 6.64% Al_2O_3	7.71	7.69			1.386	1.437		
15	Ni + Ag + 8.3% Al_2O_3	9.88	9.85			1.206	1.234		
16	Ni + Ag + 16.6% Al_2O_3	18.29				1.260	1.394		
17	Ni + Ag + 24.9% Al_2O_3	24.83	25.10			1.370	1.489		

In Table 1 the values for total impedance, as determined from at least two independent measurements using the anodes of the given compositions, are given. It can be seen from this Table that the addition of Al_2O_3 to the Ni + Ag electrodes distinctly decreases their total impedance per unit area.

As can be seen in Figs 2a and b, the specific inner surface areas of the electrodes, as determined by the BET method, are directly proportional to the concentrations of Al_2O_3 added. The slopes of the respective least square dependencies, however, differ in the case if Ni + Ag electrodes prepared by the mixing of metallic powders with solid aluminium oxide, from the slopes of the Ni + Ag electrodes saturated with the appropriate solutions and from those of pure Ni electrodes doped in the latter manner.

X-ray investigations over 1 mm^2 of the electrode area enabled a quantitative determination of the distribution of distances among the metal particles and, hence, the distribution of their sizes. From the electrodes doped with Al_2O_3 one may observe an evident disintegration of the largest Ni particles, as well as an increase in the smallest Ni particle fraction (Fig. 3). The diagrams in Fig. 4 present the distribution of distances among the Ni particles as dependent on Al_2O_3 concentration in the electrode. With increasing concentration of this compound the smallest particle fraction (0–10 μm) increases, whereas that of the largest particles (100 μm) disappears.

Some results with the addition of Al_2O_3 to the pure Ni anodes supported the conclusions concerning the role of these compounds in the performance of the anodes but, as can be seen, our pure Ni anodes had generally higher impedances and lower surface areas than the Ni + Ag ones.

4. Discussion and conclusions

Jewulski and Suski proposed a theoretical model of a MCFC porous electrode with isotropic properties [7]. This model permits the calculation of the total polarization impedance per unit geometric surface area of such electrode ($\Omega\,cm^2$) as a function of its specific internal surface area (cm^{-1}) [8]. In the above papers

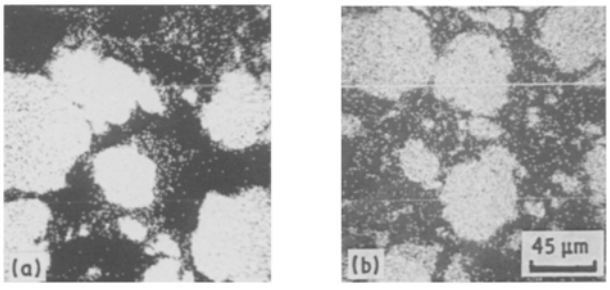

Fig. 3. X-ray detected distribution of Ni grains on the 1 mm^2 surface area of Ni + Ag electrode: (a) without Al_2O_3, (b) with 1.98 mole % of Al_2O_3.

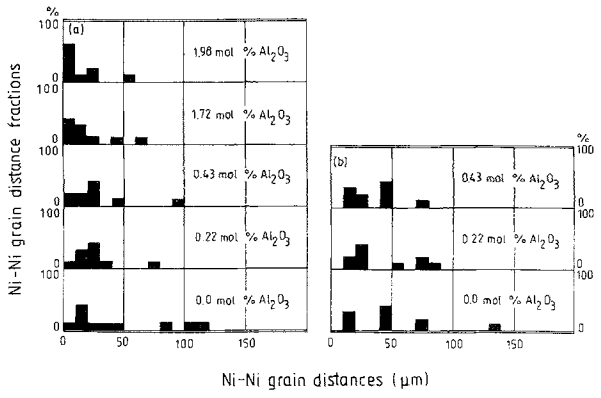

Fig. 4. Distributions of distances of nickel grains in electrodes investigated determined from X-ray microanalysis: (a) Ni + Ag electrodes doped with Al_2O_3; (b) Ni electrode doped with Al_2O_3.

the respective equations were used in a form convenient for calculations when an approximation $\kappa_M^{eff} \longrightarrow \infty$ was assumed. By this approximation the resistance of the electrode was neglected. Let us consider, however, a more general case

$$1 + [\kappa_E^{eff}/\kappa_M^{eff}] \approx 1, \quad (2)$$

where $\kappa_E^{eff} \ll \kappa_M^{eff}$ implicitly. Applying this approximation to the explicit formula for the total impedance of the electrode (Equation 6 in [8]), one gets

$$Z = \frac{\cosh(QL) + 2[\kappa_E^{eff}/\kappa_M^{eff}]}{Q\kappa_E^{eff}\sinh(QL)} + \frac{L}{\kappa_M^{eff}} \quad (3)$$

with

$$Q = [S/(Z_F\kappa_E^{eff})]^{0.5}, \quad (4)$$

For high values of the QL product

$$\cosh(QL) \approx \sinh(QL) \approx \exp(QL);$$

$$\exp(-QL) \approx 0, \quad (5)$$

and Equation 3 becomes

$$Z = (Q\kappa_E^{eff})^{-1} + L/\kappa_M^{eff}. \quad (6)$$

For low QL values we have

$$\sinh(QL) \approx QL; \quad \cosh(QL) \approx 1, \quad (7)$$

and therefore,

$$Z = (Q^2L\kappa_E^{eff})^{-1} + L/\kappa_M^{eff}. \quad (8)$$

The resulting relationship between the total impedance of the electrode and its specific internal surface takes the general form

$$Z = AS_w^{-n} + B;\ B = Z_r, \quad (9)$$

where $n = 0.5$ and $A = (Z_F \times d/\kappa_E^{eff})^{0.5}$ or $n = 1$ and $A = Z_F \times d/L$ in the case of 'ohmic' or 'microkinetic' control of the total electrode impedance, respectively. The latter case corresponds to circumstances in which the total electrode impedance is determined by the activation and/or concentration polarization of the porous electrode, the former to control by the ohmic drop in the electrolyte layer wetting the internal surface of the electrode [8]. Z_r may be equal to L/κ_M^{eff} in the case when the resistance of the sintered metallic electrode is not negligible. However, this constant may also contain the ohmic drop component of the electrode polarization as determined with respect to the reference electrode.

In order to establish whether the internal surface values per unit weight of the electrode (S_w) as determined by the BET method are related to their electrochemically active inner surfaces and whether they influence their total impedances, the results reported in Table 1 were checked in terms of Equation 9 (rearranged). Figures 5 and 6 present the experimental relationships between the parameters Z and S_w for all electrodes tested with different Al_2O_3 concentrations, for $n = 0.5$ and $n = 1$, respectively.

The least squares relationships presented in Figs 5 and 6 give the following parameters for Ni + Ag and Ni electrodes (Table 2). In these correlations the data corresponding to electrodes No. 4 (see Table 1) have not been considered. The results obtained with pure Ni + Ag electrodes do not correspond to the linear relationships in Figs 5 and 6. This irregularity is certainly not due to an experimental error. It shows that the electrodes with the internal surfaces smaller than $10^4\ cm^2\ g^{-1}$ do not obey a hyperbolic relationship with the total impedance.

As can be seen in Figs 5 and 6, a linear relationship with a higher correlation coefficient has been found in

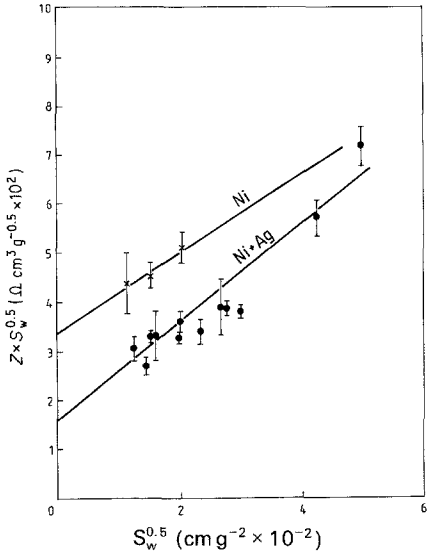

Fig. 5. Correlation of the electrode total impedances (Z) and specific inner surface areas (S_w) according to Equation 9 for $n = 0.5$: x — Ni electrodes doped with Al_2O_3; ● — Ni + Ag electrodes doped with Al_2O_3; —— least squares line.

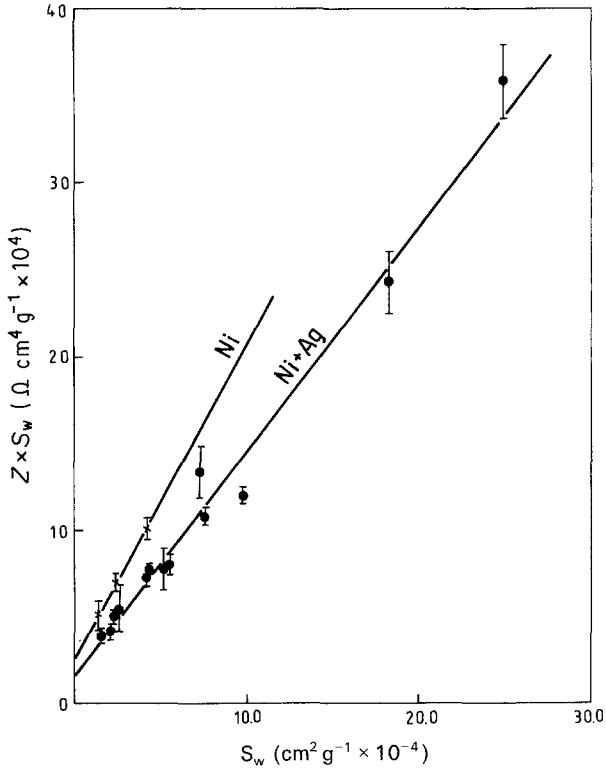

Fig. 6. Correlation of the electrode total impedances (Z) and specific inner surface areas (S_w) according to Equation 9 for $n = 1.0$: x — Ni electrodes doped with Al_2O_3, ● — Ni + Ag electrodes doped with Al_2O_3, —— least squares line.

Table 2. Least square parameters of Equation 9 (rearranged) for the Ni (1 . . . 3) and Ni + Ag (5 . . . 17) electrodes.

Electrodes tested (see Table 1)	*n*	$A \times 10^{-4n}$ $\Omega\, cm^{2(n+1)}\, g^{-n}$	B $\Omega\, cm^2$	*Correlation coefficient*
1 . . . 3	0.5	3.40 ± 0.15	0.80 ± 0.24	0.9589
5 . . . 17	0.5	1.46 ± 0.46	1.02 ± 0.12	0.9322
[1 . . . 3, 5 . . . 17	0.5	2.25 ± 0.75	0.81 ± 0.18	0.7685]
1 . . . 3	1.0	2.52 ± 0.06	1.89 ± 0.03	0.9999
5 . . . 17	1.0	1.50 ± 0.12	1.31 ± 0.05	0.9918
[1 . . . 3, 5 . . . 17	1.0	2.25 ± 1.52	1.27 ± 0.06	0.9845]

the case when $n = 1$ (kinetic control of the porous anode impedance). The values of the constant parameters, B, in Equation 9, calculated using the results for all electrodes studied, as well as for Ni and Ni + Ag electrodes separately, are much too high to be attributed to the resistance of the sintered metal only and should be interpreted as resulting from the electrolyte ohmic drop between the reference electrode and the anodes under investigation. One may conclude from Figs 2a, 2b and 6 that the impedance of the anodes under investigation is inversely proportional to their inner surface areas as determined by the BET method, i.e. to the sum of the surface areas of the porous metal and of the oxide added to the electrode.

As mentioned earlier, most of the state-of-the art models of MCFC use $LiAlO_2$ as the solid component of the electrolyte tiles, but the choice of this material is a result of purely practical tests of fuel cell performances. The above results obtained using MgO matrix electrolyte tiles have shown that small amounts of Al_2O_3 (virtually $LiAlO_2$ due to the reaction with molten lithium carbonate), develop the specific surface area of the sintered nickel anodes. The increase in this parameter takes place in two ways: (1) by the addition of the aluminium compound with a large surface area; and (2) by the dispersion of the metallic material of the electrode. The correlation presented above shows that both factors influence the performance of the electrode. We have thus shown experimentally that neither the BET Al_2O_3 surface values nor the inner surface areas of the metallic components of the electrodes show correlation according Equation 9.

Iacovangelo explained the good stability of the porous nickel MCFC anodes doped with Al_2O_3 by 'breaking' of the sintering processes taking place among the metal particles [9]. The influence of Al_2O_3 on the sintering of nickel powder has been described theoretically by Johnson [10]. The results of these authors and those obtained in the present investigation indicate that the good performance of MCFC using 'paste' electrolytes with solid $LiAlO_2$ is mainly due to the influence of aluminium compound on the internal surface areas of the porous Ni electrodes.

Acknowledgements

We wish to express our thanks to Dr L. Stachowicz for carrying out the BET measurements. Financial support from the Central R & D Project No. 3.20.59 is gratefully acknowledged.

References

[1] J. R. Selman and H. C. Maru, 'Physical Chemistry and Electrochemistry of Alkali Carbonate Metals' in 'Advances in Molten Salt Chemistry', Vol. 4 (edited by G. Mamantov and J. Braunstein), Plenum Press, New York (1981) p. 159.

[2] H. C. Maru, L. Paetsch and A. Pigeaud, 'Review of Molten Carbonate Fuel Cell Matrix Technology', Proceedings of the Symposium on Molten Carbonate Fuel Cell Technology, Vol. 84-13 (edited by J. R. Selman and T. D. Claar), The Electrochemical Society, Pennington, N.J. (1984) p. 2.

[3] G. H. J. Broers and H. J. J. van Ballegoy, 'Phase Equilibria in Li–Na–K Carbonate/Aluminate Systems', Troisièmes Journées Internationales d'Etude des Piles a Combustible. Bruxelles 16–20–VI 1969, Proceedings, Presses Academiques Europeennes, Bruxelles (1969) p. 87.

[4] G. H. J. Broers, 'The High Temperature Galvanic Cells', Doctoral thesis, University of Amsterdam, Netherlands (1958).

[5] J. Jewulski and L. Suski, 'Chemical Equilibrium Diagrams Relevant to the Molten Carbonate Fuel Cell – CHO Gas + Molten Alkali Carbonates + Metal Oxides Heterogenous System', Thermodynamical Data for Technology, Series B, Polish Scientific Publishers, Warsaw (1985).

[6] Fuel Cell Research on Second Generation Molten-Carbonate Systems, Vol. II, Project 8984, Final Status Report, Institute of Gas Technology, Chicago, Ill. (1977).

[7] J. Jewulski and L. Suski, *J. Appl. Electrochem.* **14** (1984) 135.

[8] J. Jewulski, *J. Appl. Electrochem.* **16** (1986) 643.

[9] C. D. Iacovangelo, *J. Electrochem. Soc.* **133** (1986) 2410.

[10] D. L. Johnson, *J. Mater. Sci.* **11** (1976) 2312.